

## ORIGINAL ARTICLE

# Combination therapy with anamorelin and a myostatin inhibitor is advantageous for cancer cachexia in a mouse model

Kako Hanada<sup>1</sup> | Kunpei Fukasawa<sup>1</sup> | Hiroki Hinata<sup>1</sup> | Shú Imai<sup>1</sup> |  
 Kentaro Takayama<sup>2,3</sup> | Hideyo Hirai<sup>1</sup> | Rina Ohfusa<sup>2</sup> | Yoshio Hayashi<sup>2</sup> | Fumiko Itoh<sup>1</sup> 

<sup>1</sup>Laboratory of Stem Cell Regulation, Tokyo University of Pharmacy and Life Sciences, Tokyo, Japan

<sup>2</sup>Department of Medicinal Chemistry, Tokyo University of Pharmacy and Life Sciences, Tokyo, Japan

<sup>3</sup>Department of Environmental Biochemistry, Kyoto Pharmaceutical University, Kyoto, Japan

## Correspondence

Fumiko Itoh, Laboratory of Stem Cell Regulation, Tokyo University of Pharmacy and Life Sciences, 1432-1 Horinouchi, Hachioji, Tokyo 192-0392, Japan.  
 Email: [mame.fumiko@gmail.com](mailto:mame.fumiko@gmail.com)

## Funding information

Japanese Ministry of Education, Culture, Sports, Science, and Technology, Grant/Award Number: 20K07430

## Abstract

Cancer cachexia is a multifactorial disease that causes continuous skeletal muscle wasting. Thereby, it seems to be a key determinant of cancer-related death. Although anamorelin, a ghrelin receptor agonist, has been approved in Japan for the treatment of cachexia, few medical treatments for cancer cachexia are currently available. Myostatin (MSTN)/growth differentiation factor 8, which belongs to the transforming growth factor- $\beta$  family, is a negative regulator of skeletal muscle mass, and inhibition of MSTN signaling is expected to be a therapeutic target for muscle-wasting diseases. Indeed, we have reported that peptide-2, an MSTN-inhibiting peptide from the MSTN prodomain, alleviates muscle wasting due to cancer cachexia. Herein, we evaluated the therapeutic benefit of myostatin inhibitory D-peptide-35 (MID-35), whose stability and activity were more improved than those of peptide-2 in cancer cachexia model mice. The biologic effects of MID-35 were better than those of peptide-2. Intramuscular administration of MID-35 effectively alleviated skeletal muscle atrophy in cachexia model mice, and the combination therapy of MID-35 with anamorelin increased food intake and maximized grip strength, resulting in longer survival. Our results suggest that this combination might be a novel therapeutic tool to suppress muscle wasting in cancer cachexia.

## KEYWORDS

anamorelin, cancer cachexia, muscle wasting, myostatin

## 1 | INTRODUCTION

Cancer cachexia is a severe debilitating syndrome characterized by progressive irreversible loss of skeletal muscle mass and adipose tissue in advanced cancer patients.<sup>1,2</sup> It is thought to be caused by metabolic disorders such as chronic inflammation and imbalance of skeletal

muscle synthesis/decomposition, and its etiology is difficult to clarify through pathologic and imaging examinations.<sup>3</sup> Progression of cachexia is diagnosed by the degree of unintentional weight loss and has serious impacts on the patient's QOL. Cancer cachexia develops in many advanced cancers such as gastric and lung cancers. More than 50% of patient deaths seem to be due to cancer cachexia.<sup>4</sup> To date,

**Abbreviations:** ActRIIB, activin receptor type IIB; ALK, activin receptor-like kinase; BMP, bone morphogenetic protein; CSA, cross-sectional area; EMA, European Medicines Agency; GDF, growth differentiation factor; LLC, Lewis lung carcinoma; MID-35, myostatin inhibitory D-peptide-35; MSTN, myostatin; PFA, paraformaldehyde; pSmad2, phospho-Smad2; QOL, quality of life; qPCR, quantitative PCR; SBE, Smad binding element; TGF- $\beta$ , transforming growth factor- $\beta$ .

Kako Hanada, Kunpei Fukasawa, and Hiroki Hinata contributed equally to this work.

This is an open access article under the terms of the [Creative Commons Attribution-NonCommercial-NoDerivs](https://creativecommons.org/licenses/by-nc-nd/4.0/) License, which permits use and distribution in any medium, provided the original work is properly cited, the use is non-commercial and no modifications or adaptations are made.

© 2022 The Authors. *Cancer Science* published by John Wiley & Sons Australia, Ltd on behalf of Japanese Cancer Association.

no effective medical treatment that completely improves cachexia is available, but it has been shown that adequate nutritional support and inhibition of muscle wasting can be beneficial.<sup>5</sup>

Ghrelin is a peptide hormone secreted mainly by the stomach. Increased levels of ghrelin in the body promote appetite.<sup>6,7</sup> Anamorelin is a ghrelin receptor agonist that can be taken orally.<sup>8</sup> Therefore, anamorelin augments appetite in patients with cancer cachexia, resulting in increased amounts of protein synthesis and muscle mass. Anamorelin has been shown to contribute to weight gain and to improvement of QOL in patients with non-small-cell lung cancer.<sup>9-11</sup> In a clinical trial of anamorelin, the physical function was not improved despite increased lean body mass in cancer cachexia patients. Therefore, the EMA rejected use of this medicine for clinical therapy, whereas Japan has approved it.

Myostatin (GDF-8), activin-A, and GDF-11, which belong to the TGF- $\beta$  family, are known to negatively regulate skeletal muscle mass in humans and animals.<sup>12-16</sup> Myostatin is initially produced as a latent form by cells, then it undergoes proteolytic cleavage to become an active ligand. After the mature MSTN binds to the type I (ALK4/5) and type II (ACTRIIa/b) serine/threonine kinase receptors, the type I serine/threonine kinase receptor phosphorylates Smad2 and Smad3 to transduce its signals.<sup>17</sup> Deficiency of MSTN signaling showed a hypermuscular phenotype with increased muscle mass<sup>18</sup>; in addition, inhibition of MSTN and activin-A signaling is effective against cancer cachexia.<sup>16,19,20</sup>

We have reported that peptide-2, an MSTN inhibitory region from the mouse MSTN prodomain, was able to alleviate muscle wasting in cancer cachexia model mice. By improving the activity and stability of peptide-2,<sup>21-23</sup> we have developed MID-35 (IC<sub>50</sub> value of 0.19  $\mu$ M, Figure S1), which is approximately 20 times more active than peptide-2 (IC<sub>50</sub> = 4.1  $\mu$ M). In this study, we examined the effect of MID-35 or its combination with anamorelin on muscle wasting observed in cancer cachexia model mice.

## 2 | MATERIALS AND METHODS

### 2.1 | Cell culture

HepG2 and LLC cells were cultured in DMEM (Nacalai Tesque) containing 10% FCS (Invitrogen), 1 $\times$ MEM nonessential amino acids (Nacalai Tesque), and 100U/ml penicillin/streptomycin (Wako). C2C12 cells were cultured in the same media except for 15% FCS instead of 10% FCS. When they had differentiated into myoblasts, the C2C12 cells were cultured in DMEM containing 2% horse serum (Cosmo Bio Co., Ltd), nonessential amino acids, and penicillin/streptomycin.

### 2.2 | Drugs

MID-35 synthesis was described previously.<sup>24</sup> MID-35 and SB-431542 (Sigma-Aldrich) were reconstituted in saline and DMSO, respectively. Anamorelin (Aadoo Bioscience) was dissolved in sterile

water. The dosage of anamorelin (30 mg/kg) was determined according to a previous study.<sup>25</sup>

### 2.3 | Smad-dependent transcriptional reporter assay

HepG2 cells were transfected in a 24-well plate with (SBE)<sub>4</sub>-luc and pCH110 (GE Healthcare Bioscience) as described previously.<sup>20</sup> Where indicated, 10 ng/ml MSTN, 10 ng/ml GDF-11, 5 ng/ml activin-A, or 5 ng/ml TGF- $\beta$  was added to the wells after the cells had been pretreated with MID-35 (3  $\mu$ M) or SB-431542 (10  $\mu$ mol/L) for 1 h.<sup>26,27</sup> Subsequently, the cells were cultured for 8 h with or without ligands. The luciferase activity of the cells was then measured, as was the  $\beta$ -galactosidase activity, which was used to normalize the transfection efficiency. All the ligands were purchased from Wako. Each transfection was carried out in triplicate and repeated at least twice. Values are expressed as mean  $\pm$  SD ( $n = 3$ ).

### 2.4 | Animal studies

Male C57BL/6J mice (8-12 weeks old; 20-24 g) were purchased from Charles River Laboratories, and fed a standard laboratory diet and housed in a temperature-controlled room under specific pathogen-free conditions. An anesthetic mixture consisting of 0.3 mg/kg medetomidine, 4.0 mg/kg midazolam, and 5.0 mg/kg butorphanol was administered. For the cancer cachexia model, LLC cells ( $5 \times 10^5$  cells in 100  $\mu$ l saline) were subcutaneously injected around the dorsal butt of C57BL/6J mice after anesthesia.<sup>28</sup> For ethical reasons, we decided on the end-point of the cancer cachexia model as 22 or 20 days after inoculation of the cells. Some mice died of natural causes, while the rest were euthanized when they showed signs of morbidity according to the experimental animal guidelines (e.g., emaciation, lethargy or failure to respond to gentle stimuli, or hypothermia). We undertook the mouse experiments in accordance with the institutional guidelines of the Animal Care and Use Program of the Tokyo University of Pharmacy and Life Sciences (L20-5, L21-7). The total four-limb grip strength for each mouse was measured as described previously.<sup>20</sup>

### 2.5 | Western blot analysis

Western blot analysis was carried out as described previously.<sup>20,28,29</sup> Antibodies were obtained from the following sources: mouse anti-Smad2/3 mAb (cat. 610843, 1:1000) from BD Transduction Laboratories, mouse monoclonal anti- $\beta$ -actin (sc-69879, 1:5000) from Santa Cruz Biotechnology, rabbit polyclonal pSmad2 Ab, termed PS2 (1:1000) was homemade, and HRP-conjugated goat anti-rabbit or anti-mouse IgG Abs (NA931V and NA934V, respectively, 1:10000) from Amersham Pharmacia. The nitrocellulose membranes (Santa Cruz Biotechnology) were probed with the indicated Abs. Primary Abs were detected with HRP-conjugated Ab with a chemiluminescent substrate (Thermo Fisher Scientific).

## 2.6 | Immunofluorescence analysis and quantification

To detect the formation of myotubes in differentiated C2C12 cells, filament actin was stained with rhodamine-phalloidin (Sigma). Four days after the induction of myoblast differentiation, the cells were rinsed with PBS, fixed with 4% PFA, and permeabilized with 0.1% polyoxyethylene (10) octylphenyl ether (Wako) for 10 min. The cells were washed with PBS three times and then stained with 200 ng/ml phalloidin and CF568 conjugate (cat. 00044; Biotium, Inc.) for 30 min. To determine the diameter of the C2C12 myotubes, at least 20 myotubes were measured per sample cultured in differentiation medium with ImageJ.

The gastrocnemius muscles were surgically removed and embedded into frozen section compound (Leica Camera). Fresh-frozen sections (5  $\mu$ m) were cut with a CM1850 cryostat (Leica), mounted on cryofilm (Leica) and fixed in 100% ethanol, followed by fixation in 4% PFA. The films were washed three times with PBS, permeabilized with 0.1% polyoxyethylene (10) octylphenyl ether (Wako), blocked with blocking solution (Vector Laboratories) for 1 h at 37°C, and incubated with the first Ab in the blocking solution overnight at 4°C. The films were washed three times with PBS and then incubated with Alexa488-conjugated donkey anti-rabbit IgG (A21206; Thermo Fisher Scientific) or Alexa594-conjugated goat anti-rabbit IgG (A21207; Thermo Fisher Scientific) Ab at 1:200 for 1 h at room temperature. For mouse-on-mouse staining, an MOM immunodetection kit (FMK-2201; Vector Laboratories) was used. After the nuclei were stained with 2  $\mu$ g/ml DAPI for 10 min, the films were mounted with mounting medium (Dako). To visualize the fluorescence, a BZ-9000 fluorescence microscope (Keyence) was used. Smad2/3 nuclear accumulation from each mouse ( $n = 2$ ) was calculated with the rate of DAPI and Smad2/3-positive cells from at least 50 dystrophin-positive nuclei per mouse.

## 2.7 | RNA isolation and quantitative real-time RT-PCR

Total RNA was isolated using a ReliaPrep RNA Cell Miniprep System (Promega). Reverse transcription was carried out with a PrimeScript II 1st strand cDNA Synthesis Kit (Takara Bio Inc.). Quantitative PCR was undertaken using a THUNDERBIRD SYBR qPCR Mix Fast qPCR kit (TOYOBO Co., Ltd) with LightCycler 96 (Roche). Each sample was analyzed in triplicate at least twice for each qPCR measurement. The sequences of the primers used are listed in Table S1.

## 2.8 | Cell viability assay

LLC cells were cultured with anamorelin or MID-35 for 24 h. The concentration of anamorelin is based on the plasma  $C_{\max}$  average (707  $\pm$  307 ng/ml) of men who received 100 mg in a clinical trial. The viability of LLC cells was assessed by using the CellTiter-Glo 2.0

(Promega), following standard material procedures. Values were expressed as mean  $\pm$  SD ( $n = 3$ ).

## 2.9 | Statistical analysis

Numeric results are expressed as mean  $\pm$  SD. Significance was assessed using the unequal variances t-test and the  $\chi^2$ -test. Probability values below 0.05, 0.01, and 0.001 were considered significant.

# 3 | RESULTS

## 3.1 | Inhibitory effects of MID-35 on TGF- $\beta$ family signaling

MID-35, composed of only 16 amino acids, is able to inhibit MSTN signaling.<sup>24</sup> To characterize the inhibitory effect of MID-35 on TGF- $\beta$ , activin, and GDF-11 signaling in addition to MSTN signaling, we undertook a luciferase assay using the (SBE)<sub>4</sub>-luc reporter.<sup>30</sup> Cells were stimulated with each ligand 8 h after being preincubated with MID-35 or SB-431542, which is a known kinase inhibitor for ALK4, ALK5, and ALK7 kinases,<sup>26</sup> for 1 h. MID-35 inhibited TGF- $\beta$ - and GDF-11-induced reporter activity in addition to MSTN-induced transcriptional activity, whereas SB-431542 suppressed the luciferase activities induced by all the ligands used (Figure 1A,B). To investigate whether MID-35 can perturb phosphorylation of Smad2 by MSTN or TGF- $\beta$ , C2C12 cells were stimulated with the ligands for 1 h. Myostatin- or TGF- $\beta$ -mediated Smad2 phosphorylation was marginally decreased in the presence of MID-35, whereas it was completely inhibited in the presence of SB-431542 (Figure 1C,D). Subsequently, we investigated whether the nuclear translocation of Smad2 was inhibited by MID-35 when the cells were stimulated with MSTN. Like SB-431542, MID-35 completely blocked their nuclear accumulation (Figure 1E). These results indicated that MID-35 is capable of inhibiting the Smad2 signaling pathways mediated by MSTN.

## 3.2 | Inhibitory effect of MID-35 on MSTN-mediated inhibition of myoblast differentiation

Next, we examined whether MID-35 enhanced differentiation of C2C12 myoblasts through its inhibitory activity of MSTN signaling. When C2C12 cells were cultured in differentiation medium with 2% horse serum<sup>31</sup> for 4 days, the cells showed syncytial myotubes. After the cells were stained with rhodamine-labeled phalloidin, we could detect cell fusion and small muscle fiber formation (Figure 2A). The treatment of cells with MSTN showed suppression of cell differentiation. Both MID-35 and SB-431542 lifted MSTN-mediated inhibition of cell differentiation (Figure 2B). We further investigated the effect of MID-35 on mRNA expression of muscle creatine kinase (MCK), myosin light chain (MyIpf), and

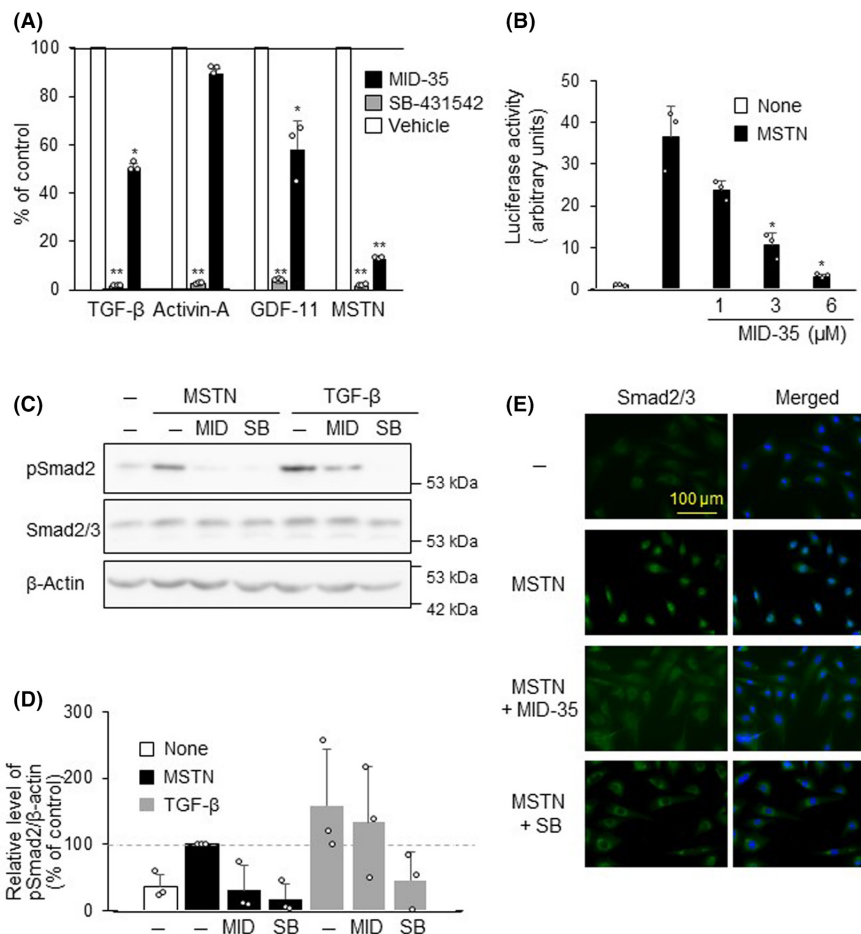


**FIGURE 1** Myostatin inhibitory D-peptide-35 (MID-35) inhibits myostatin (MSTN) signaling. (A,B) HepG2 cells transfected with an (SBE)<sub>4</sub>-luc reporter construct were stimulated with transforming growth factor- $\beta$  (TGF- $\beta$ ; 5 ng/ml), activin-A (10 ng/ml), growth differentiation factor-11 (GDF-11; 10 ng/ml), or MSTN (10 ng/ml), and the reporter activity was measured. These ligands preincubated with MID-35 (3  $\mu$ M) or SB-431542 (10  $\mu$ M) (A) or MID-35 (1, 3, or 6  $\mu$ M) (B) were added to the cells for 8 h. Inhibition efficiency is shown as the percentage of control. All values represent the mean  $\pm$  SD ( $n = 3$ ). (C) MID-35 inhibited MSTN-induced Smad2 and Smad3 phosphorylation. MID-35 (MID; 3  $\mu$ M) or SB-431542 (SB; 10  $\mu$ M) were preincubated with MSTN (10 ng/ml) or TGF- $\beta$  (5 ng/ml) for 1 h and added to C2C12 cells for 1 h. These cell lysates were subjected to western blot analysis using anti-phospho-Smad2 (pSmad2), anti-Smad2/3, and anti- $\beta$ -actin Abs. (D) Quantification for pSmad2 protein levels was normalized using the intensity of the band corresponding to  $\beta$ -actin. Each relative intensity was calculated by comparing it with the value for the MSTN-stimulated cells. (E) Smad2/3 nuclear localization induced by MSTN was inhibited by MID-35. Immunofluorescence staining for Smad2/3 (green) in C2C12 cells. MID-35 (MID; 3  $\mu$ M) or SB-431542 (SB; 10  $\mu$ M) was preincubated with MSTN (10 ng/ml) for 1 h, and added to C2C12 cells for 1 h. Nuclei were counterstained with DAPI (blue).

myogenin, all of which are known to be expressed in myotubes (Figure 2C). Myostatin attenuated the transcripts of these marker genes, although each of these genes was highly upregulated in the differentiation medium. MID-35 and SB-431542 slightly and completely inhibited the inhibitory action of MSTN, respectively (Figure 2C). We further confirmed the reduced mRNA expression of MSTN, whose expression is known to be suppressed by the induction of myotube differentiation<sup>32</sup> (Figure S2).

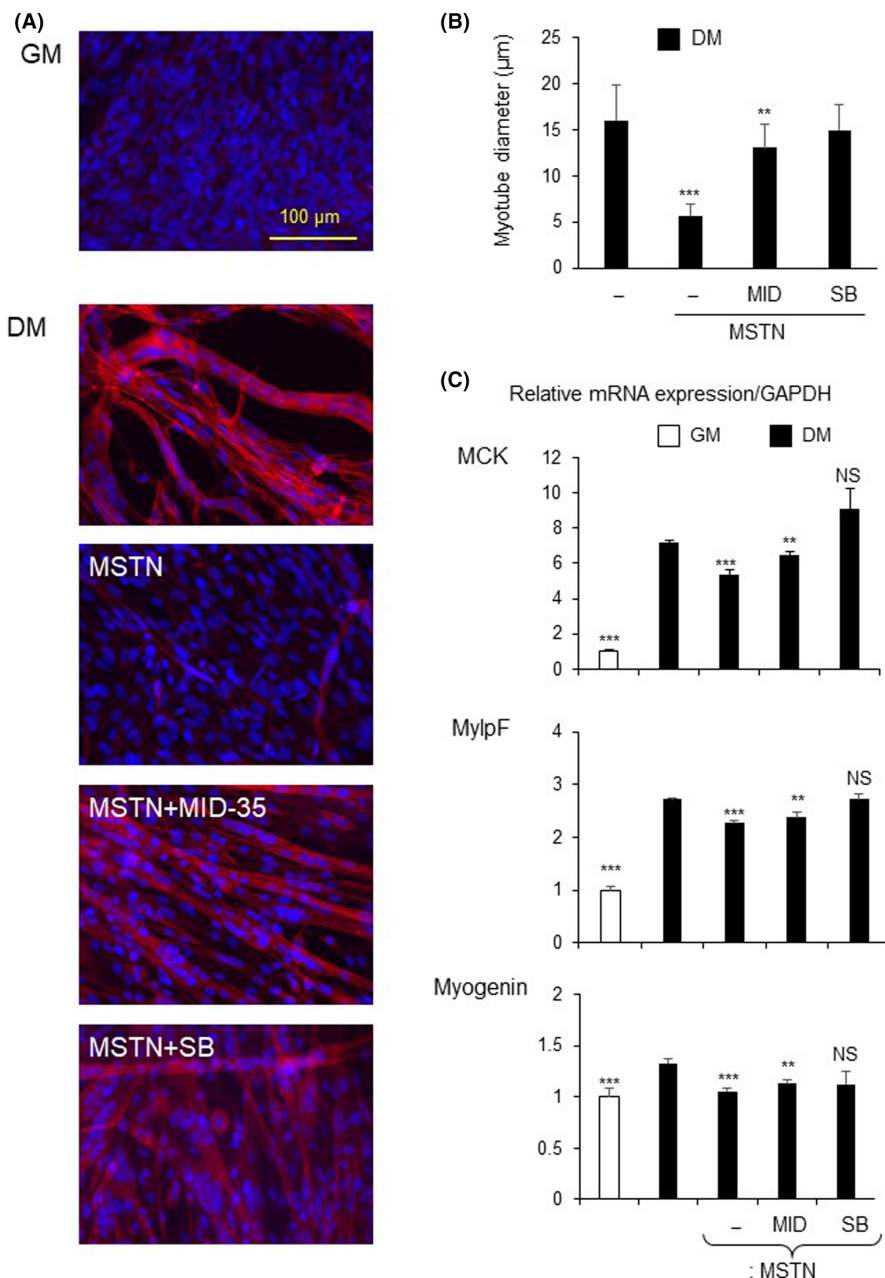
### 3.3 | Alleviation of muscle wasting in cancer cachexia model mice treated with MID-35

To investigate the *in vivo* effect of MID-35 on cancer cachexia, LLC cells were subcutaneously inoculated into the dorsal butt of anesthetized C57BL/6 mice. MID-35 was administered to mouse

gastrocnemius muscle 4, 11, and 18 days after the transplantation of the cells (Figure 3A). MID-35 did not affect the survival ratio (Figure 3B), body weight change (Figure 3C), cancer growth (Figure 3D,E), or heart weight per body weight without tumor (Figure 3F) in the cancer cachexia model mice. However, the MID-35-treated mice showed a significantly higher percentage of subcutaneous fat weight per body mass without tumor than the PBS-treated mice (Figure 3G). This result indicates that MID-35 was effective in treating cancer cachexia model mice when compared with peptide-2, which did not improve loss of fat weight.

Like the subcutaneous fat weight in MID-35-treated mice, their gastrocnemius muscles augmented 22 days after transplantation of LLC cells (Figure 4A,B). Next, the gastrocnemius muscle cross-sections were stained with an anti-dystrophin Ab (Figure 4C). The muscle fiber area from the PBS-treated mice ( $1415.3 \pm 504.7 \mu\text{m}^2$ ) revealed a reduction of 22.1% when compared with that from the

**FIGURE 2** Myostatin inhibitory D-peptide-35 (MID-35) inhibited the effect of myostatin (MSTN) and promoted C2C12 myoblast differentiation. (A) C2C12 cells in growth medium (GM), which was replaced with differentiation medium (DM) (2% horse serum [HS]) containing MSTN (10 ng/ml), MID-35 (MID; 3  $\mu$ M), or SB-431542 (SB; 10  $\mu$ mol/L), as described, for 4 days. These cells were stained with TRITC-phalloidin (red) and DAPI (blue). (B) Diameters of C2C12 myotubes. Significance was compared with the DM without MSTN. (C) Results from quantitative PCR analysis of the C2C12 differentiation markers muscle creatine kinase (MCK), myosin light chain (MyIpF), and myogenin in C2C12 cells 4 days after the induction of differentiation. Data are expressed as mean  $\pm$  SD ( $n = 3$ ). \*\* $p < 0.01$ ; \*\*\* $p < 0.001$ . NS, not significant.



healthy control mice ( $1817.2 \pm 502.0 \mu\text{m}^2$ ), whilst the MID-35-treated mice ( $1658.4 \pm 424.3 \mu\text{m}^2$ ) showed a reduction of 8.2%. The boxplot analyses indicated that MID-35 improved the fiber size in muscles (Figure 4D). Furthermore, the grip strength in mice treated with MID-35 was significantly increased when compared with that in control mice (Figure 4E). These results indicate that MID-35 might be able to retard the progression of cancer cachexia.

### 3.4 | Effect of combination therapy of MID-35 with anamorelin on cancer cachexia model mice

Anamorelin is an orally administrable ghrelin receptor agonist that is useful for cancer cachexia. Therefore, we investigated how the combined treatment of MID-35 with anamorelin affects symptoms in cancer

cachexia model mice (Figure 5A). As shown in Figure 5(B), the combination therapy showed a better survival rate than either MID-35 or anamorelin alone ( $p = 0.052$ ,  $\chi^2$ -test). The body weights among the groups examined were not altered (Figure 5C), although the mice treated with the combination therapy tended to have larger tumor volumes than did the PBS-treated mice ( $p = 0.09$ ; Figure 5D,E). Neither anamorelin nor MID-35 had an effect on promoting growth of LLC cells (Figure S3). Indeed, among the groups examined, the mice treated with the combination therapy took food and water the most often (Figure 5F,G). The percentage of heart weight per body mass without tumor weight did not differ among the groups examined (Figure 5H), whereas the proportion of subcutaneous fat in the mice treated with the combination therapy increased (Figure 5I). These results suggested that the combination therapy of MID-35 with anamorelin might be more effective against cancer cachexia than MID-35 or anamorelin alone.

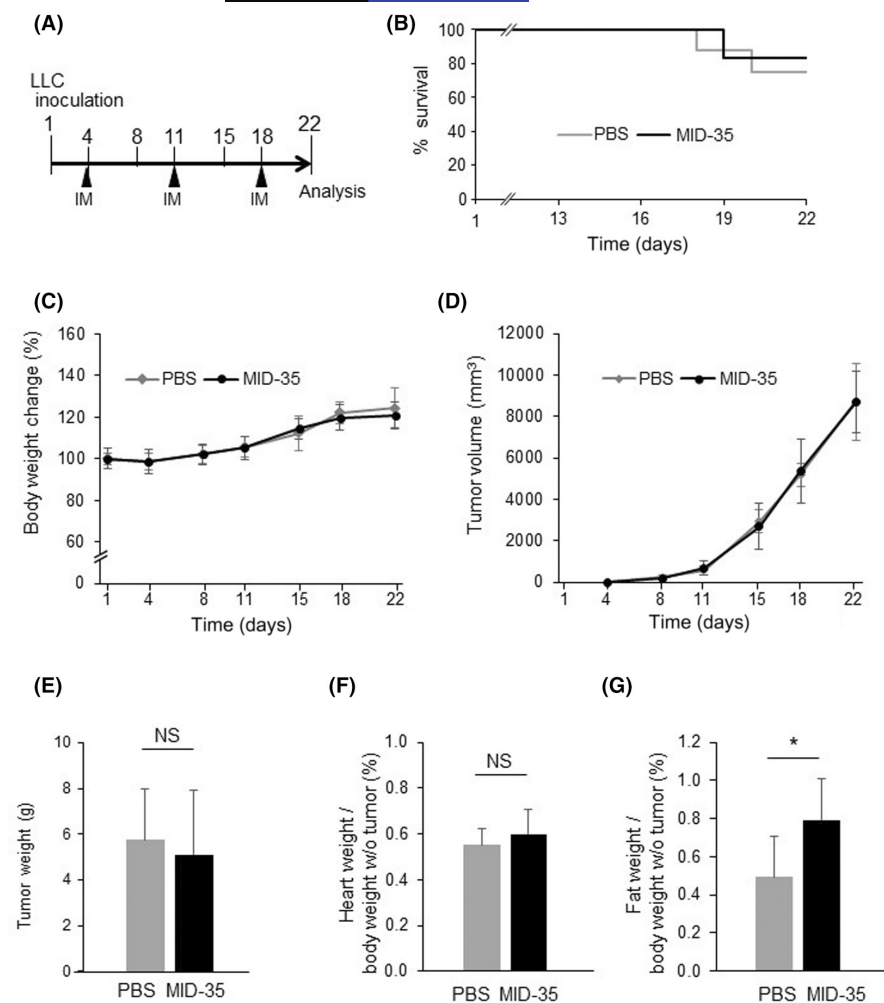


**FIGURE 3** Myostatin inhibitory D-peptide-35 (MID-35) did not affect tumorigenesis. (A) Schematic diagram of the experimental schedule. Day 1: Lewis lung carcinoma (LLC) cell inoculation. Days 4, 11, and 18: intramuscular administration (IM) of MID-35 (30 nmol/leg) or PBS (30  $\mu$ l/leg). (B) Survival rates of LLC-bearing mice treated with MID-35 or PBS were analyzed. (C,D) Changes in relative body weights based on the day 1 (C) and estimated tumor volume in LLC-bearing mice. Tumor volumes were calculated using the formula: length  $\times$  width  $\times$  width  $\times$  0.5. (E–G) Tumor weight (E), heart weight/body weight without (w/o) tumor weight (F), and subcutaneous fat weight/body weight w/o tumor weight (G) were measured. Data are expressed as mean  $\pm$  SD ( $n = 6$ ). \* $p < 0.05$ . NS, not significant.

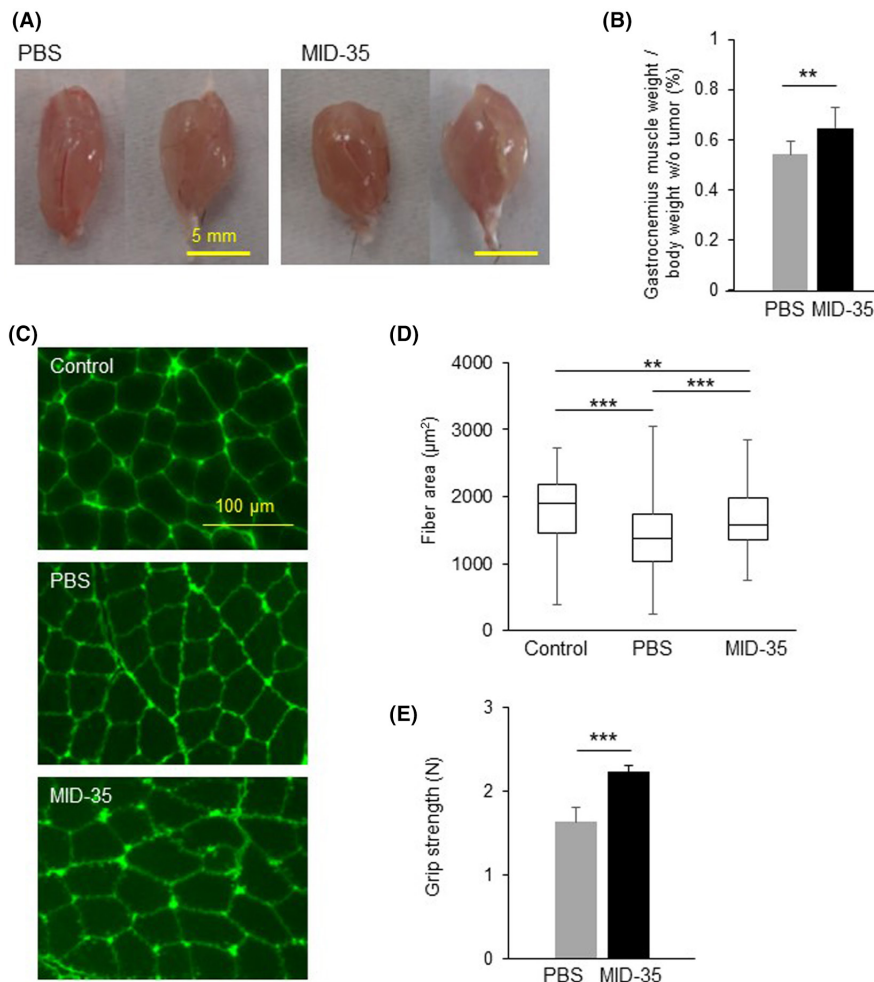
When we observed the gastrocnemius muscles from each mouse 22 days after the transplantation of LLC cells, the muscle atrophy in the PBS-treated mice was the most remarkable among the mice examined (Figure 6A,B). The gastrocnemius weight per body weight without tumor increased in the mice treated with anamorelin alone, MID-35 alone, or the combination of MID-35 with anamorelin, although the combination therapy was the most effective among the treatments (Figure 6B). Consistent with this result, the combination therapy showed the maximum grip strength (Figure 6C). Therefore, the cross-sections of the gastrocnemius muscles from the cancer cachexia model mice and the control mice were stained with an antidystrophin Ab. When the size of muscle fibers was evaluated using frequency distribution (Figure S3) and boxplot (Figure 6D) analyses, the MID-35-treated mice showed the highest value among the mice examined. To investigate whether the improvement in muscle atrophy was mediated through the inhibition of the MSTN/Smad signaling pathway, immunohistological analysis of the gastrocnemius muscle was carried out to detect nuclear accumulation of Smad2/3 (Figure 6E). Compared with the control healthy mice, the PBS-treated mice showed increased Smad2/3 nuclear translocation, although we could see a decrease of nuclear translocation of Smad2/3 in the mice treated with MID-35 and/or anamorelin. In particular, it was found that MID-35 was the strongest in terms of reduction

of nuclear translocation of Smad2/3, suggesting that MID-35 effectively suppressed MSTN/Smad2/3 signaling (Figure 6E). To confirm whether inhibition of Smad2/3 nuclear translocation affects muscular atrophy, we investigated mRNA expression of the muscle atrophy markers<sup>33</sup> muscle RING finger 1 (MuRF1)/Trim63, F-box only protein 31 (Fbxo31), and muscle atrophy F-box (MAFbx)/atrogen-1. These expressions were significantly increased in the gastrocnemius muscle in mice bearing cancer when compared with those in healthy control mice. In particular, MID-35 most effectively suppressed the expression of these genes (Figure 6F). Contrary to our expectations, there was no synergistic effect between MID-35 and anamorelin related to these mRNA expressions. These results might be due to differing effects of MID-35 and anamorelin on muscle atrophy.

## 4 | DISCUSSION

Cancer cachexia leading to severe weight loss and anorexia is a multifactorial syndrome that develops in many types of cancer and chronic inflammatory diseases. In cancer cachexia patients, weight loss is due to atrophy of the skeletal muscles, unlike malnutrition which affects the adipose tissues. Myostatin, GDF-11, activin, and TGF- $\beta$  are known as potential factors that exacerbate skeletal

**FIGURE 4** Myostatin inhibitory D-peptide-35 (MID-35) alleviates muscle wasting in cancer cachexia model mice. (A) Photographs of gastrocnemius muscle of cancer cachexia mice in Figure 3. (B) Gastrocnemius muscle weight/body weight without (w/o) tumor weight. (C) Representative immunofluorescence analysis of dystrophin-stained gastrocnemius sections from the indicated groups. Cryosections were stained with antidystrophin Ab (green). (D) Box and whisker plots show the distribution of the muscle fiber cross-sectional area from three identical images for each group ( $n = 3$ ). (E) Grip strength analysis of cachexic mice treated with PBS or MID-35. Data are expressed as mean  $\pm$  SD ( $n = 6$ ). \*\* $p < 0.01$ ; \*\*\* $p < 0.001$ .



muscle atrophy. These cytokines can promote phosphorylation of both Smad2 and Smad3, whereas their phosphorylation status was diverse (Figure 1C) because of the different expression levels of their receptors on the cell membrane.<sup>34</sup> Therefore, simultaneous inhibition of these factors is preferred to suppression of MSTN alone for muscle-wasting diseases. In this study, we showed that MID-35, possessing a stable structure in vivo, can inhibit TGF- $\beta$  and GDF-11 signaling as well as MSTN signaling. The broad spectrum of TGF- $\beta$  family signaling might be beneficial to improvement of muscle wasting in cancer cachexia (Figure 5).<sup>35</sup>

Suppression of MSTN and activin-A expression as well as inhibition of their function is known to prompt increase in muscle mass. Activin is produced from a variety of cell types, whereas MSTN is primarily synthesized by skeletal muscle cells to act in an autocrine loop. Systemic treatment with soluble ActRIIB-Fc reportedly had a therapeutic potential on cancer cachexia model mice.<sup>16</sup> However, ActRIIB also binds to both BMP9 and BMP10, which regulate vascular function through Smad1/5/8, causing vascular side-effects.<sup>36</sup> In this study, we showed that MID-35 does not affect activin signaling. Therefore, it might show a therapeutic effect on muscle fiber hypertrophy in addition to alleviation of muscle wasting in cancer cachexia. No vascular abnormalities such as bleeding were observed when MID-35 was injected into hind legs. Although atrophy of

skeletal muscles can be seen throughout the body of patients with cancer cachexia, it is possible that local intramuscular administration of MID-35 might be enough to improve their QOL because increase of muscle mass in patients with tumors is known to prolong their survival.<sup>37</sup>

MID-35 is a retro-inverso peptide that consists of a linear structure with a reversed amino acid sequence including D-amino acids, rendering it resistant to proteolysis.<sup>24</sup> Intramuscular administration of MID-35 significantly enhanced gastrocnemius weight per body weight in cancer cachexia mice (Figure 4B). Compared with peptide-2, MID-35 significantly improved atrophied muscle fiber as shown on cross-sections (Figures 4D and 6D) and increased fat proportion (Figure 3G) in cachexia model mice.

Anamorelin, an orally administrable ghrelin receptor agonist, is expected to improve the appetite of patients with cancer cachexia and to increase their weight.<sup>6-8</sup> It has been approved in Japan for the treatment of cancer cachexia patients with malignant non-small-cell lung, gastric, pancreatic, or colorectal cancer. However, the EMA and the FDA have not yet approved the use of anamorelin for cancer cachexia patients. Although there are no suitable ways to evaluate muscle function in humans, we were able to evaluate the quality and function of mouse muscles by measuring the CSA and grip strength, respectively. MID-35 counteracted muscle

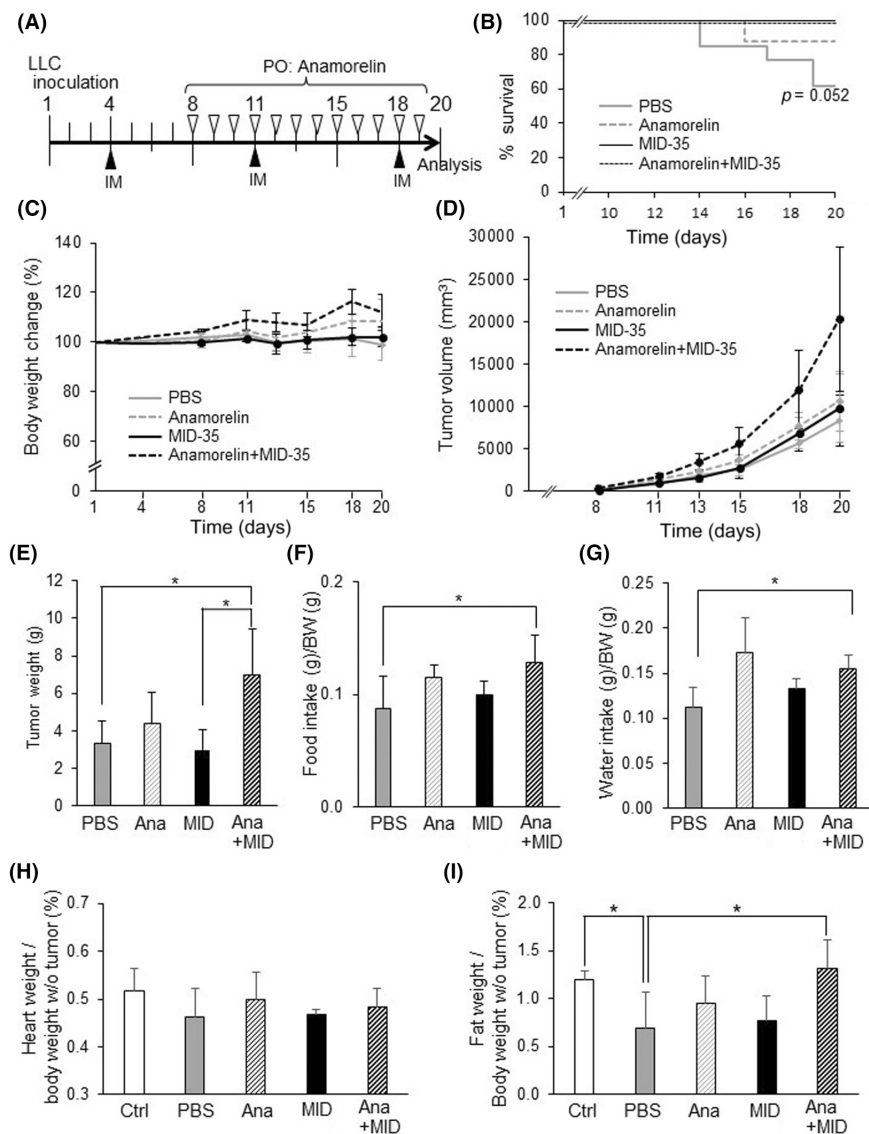


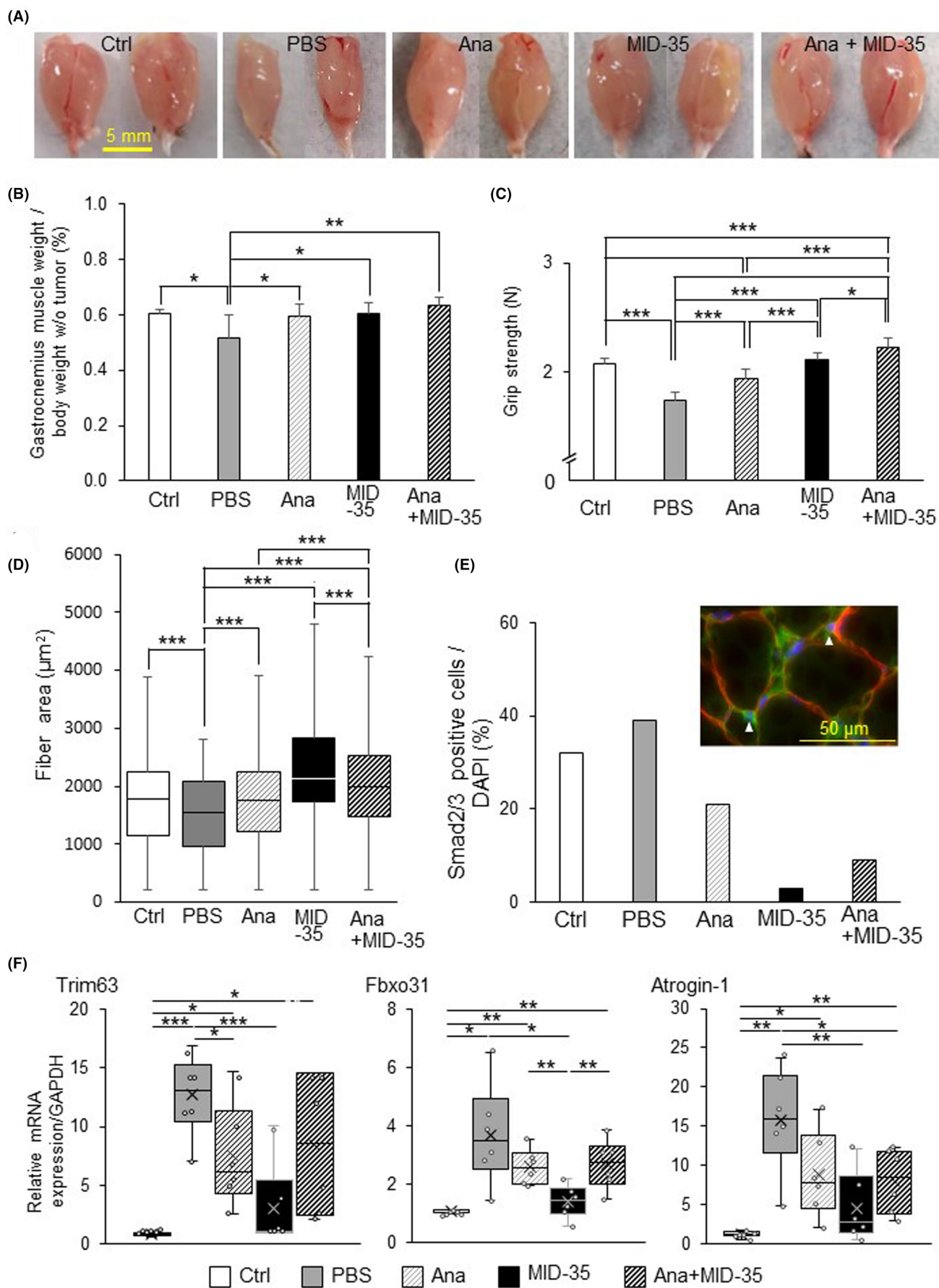
**FIGURE 5** Combination of myostatin inhibitory D-peptide-35 (MID-35) and anamorelin improves survival in cancer cachexia model mice. (A) Schematic diagram of the experimental schedule. Day 1: Lewis lung carcinoma (LLC) cell inoculation. Days 4, 11, and 18: intramuscular administration (IM) of MID-35 (MID; 30 nmol/leg) or PBS (30  $\mu$ l/leg). Days 8–19: per oral administration (PO, 10 ml/kg) of anamorelin (Ana; 3 mg/ml) or water ( $n = 6$ ). (B) Survival rates of LLC-bearing mice with MID-35 or PBS treatment were analyzed ( $n = 6$ ). (C,D) Changes in relative body weights (BW) based on the first day (C) and estimated tumor volume in LLC-bearing mice (D) ( $n = 6$ ). (E–G) Tumor weight (E), food intake (F), water intake (G), heart weight/body weight without (w/o) tumor weight (H), and subcutaneous fat weight/body weight w/o tumor weight (I) from the indicated groups were measured. Data are expressed as mean  $\pm$  SD ( $n = 6$ ). \* $p < 0.05$ .

atrophy in mice with tumors (Figures 4A and 6A) in addition to enlarging the CSA in muscles of mice with tumors. In our current study, combination therapy with MID-35 and anamorelin showed the most potent grip strength among the treatments examined, although anamorelin or MID-35 alone alleviated CSA atrophy in the cancer cachexia model mice. To our knowledge, this is the first study to examine the combination treatment of anamorelin with the MSTN inhibitor in cancer cachexia model mice. Whether this combination therapy will improve mouse QOL must be further evaluated in the future. Unfortunately, the combination therapy

maximized tumor size in mice with tumors (Figure 5D). Tumor growth with the combination therapy would be due to the synergistic effect of increase food intake by improved appetite and athletic performance. In human patients, it was reported that providing nutritional support caused tumor growth.<sup>38</sup> We speculated that the mice could take a large amount of food and water (Figure 5G,F) because of improvement of their QOL. Thus, we supposed that they could survive longer, although their tumors could grow as well. Since the combination therapy of anamorelin with MID-35 possesses growth-promoting effect on tumors, it is

**FIGURE 6** Combination of myostatin inhibitory D-peptide-35 (MID-35) with anamorelin (Ana) improves survival in cancer cachexia model mice. (A) Photographs of gastrocnemius muscle of cancer cachexia mice in Figure 5. (B) Gastrocnemius muscle weight/body weight without (w/o) tumor weight. (C) Grip strength analysis of cachexic mice from the indicated groups. (B,C) Data are expressed as mean  $\pm$  SD. (D) Box and whisker plots show the distribution of the muscle fiber cross-sectional area for each group. (E) Percentage of gastrocnemius Smad2/3 nuclear translocation. Cryosections were stained with anti-Smad2/3 (green), antidyostrophin (red), and DAPI (blue) ( $n = 2$ , each group). Representative image of Smad2/3 translocation (arrowheads) from control mice is shown. (F) Results from quantitative PCR analysis of the muscle atrophy markers Trim63, F-box only protein 31 (Fbxo31), and atrogen-1 in gastrocnemius muscle from the indicated groups. Data are shown in whisker plots ( $n = 6$  mice/group). \*\*\* $p < 0.001$ ; \*\* $p < 0.01$ ; \* $p < 0.05$ .





necessary to further evaluate the combination therapy accompanied with surgical operation, chemotherapy, or radiation therapy.

In summary, MID-35 might be useful as a therapeutic drug for patients with muscle-wasting diseases such as cancer cachexia and sarcopenia because of its improvement of muscle atrophy. Furthermore, we have shown that the combination treatment of MID35 with anamorelin administered to cancer cachexia model mice showed enhancement of appetite, thus improving the general health as well as muscle quality of the mice. We suppose that both improvement of muscle function and chemotherapy are needed to improve the QOL of patients with tumors.

#### AUTHOR CONTRIBUTIONS

KH, KF, HH, SI, and FI conducted the in vivo and in vitro experiments and analyzed the data. KT, HH, RO, and YH took part in the interpretation of the data and discussion of the paper. FI wrote the manuscript. FI, KH, KT, HH, and YH revised the manuscript. All authors have read and approved the manuscript.

#### ACKNOWLEDGMENTS

This research was supported by the Japanese Ministry of Education, Culture, Sports, Science, and Technology (20K07430 to F.I.). We thank Dr. S. Itoh for his marvelous advice. We would like to thank Flaminia Miyamasu for English language editing.

#### FUNDING INFORMATION

Japanese Ministry of Education, Culture, Sports, Science, and Technology, Grant/Award Number: 20K07430.

#### DISCLOSURE

The authors have no conflicts of interest.

#### ETHICS STATEMENT

The research protocol was approved by an institutional review board (L20-5, L21-7).

#### ANIMAL STUDIES

The mouse experiments were carried out in accordance with the institutional guidelines of the Animal Care and Use Program of the Tokyo University of Pharmacy and Life Sciences (L20-5, L21-7).

#### ORCID

Fumiko Itoh  <https://orcid.org/0000-0002-6134-5331>

#### REFERENCES

1. Fearon K, Arends J, Baracos V. Understanding the mechanisms and treatment options in cancer cachexia. *Nat Rev Clin Oncol*. 2013;10:90-99.
2. Cole CL, Kleckner IR, Jatoi A, Schwarz EM, Dunne RF. The role of systemic inflammation in cancer-associated muscle wasting and rationale for exercise as a therapeutic intervention. *JCSM Clin Rep*. 2018;3(2):e00065.
3. Fearon K, Strasser F, Anker SD, et al. Definition and classification of cancer cachexia: an International consensus. *Lancet Oncol*. 2011;12:489-495.
4. Baracos VE, Martin L, Korc M, Guttridge DC, Fearon KCH. Cancer-associated cachexia nature reviews disease primers. *Nat Rev Dis Primers*. 2018;4:17105.
5. van de Worp W, Schols A, Theys J, van Helvoort A, Langen RC. Nutritional interventions in cancer cachexia: evidence and perspectives from experimental models. *Front Nutr*. 2020;7:601329.
6. Kojima M, Hosoda H, Date Y, Nakazato M, Matsuo H, Kangawa K. Ghrelin is a growth-hormone-releasing acylated peptide from stomach. *Nature*. 1999;402:656-660.
7. Sun Y, Garcia JM, Smith RG. Ghrelin and growth hormone secretagogue receptor expression in mice during aging. *Endocrinology*. 2007;148:1323-1329.
8. Anker SD, Coats AJ, Morley JE. Evidence for partial pharmaceutical reversal of the cancer anorexia-cachexia syndrome: the case of anamorelin. *J Cachexia Sarcopenia Muscle*. 2015;6:275-277.
9. Katakami N, Uchino J, Yokoyama T, et al. Anamorelin (ONO-7643) for the treatment of patients with non-small cell lung cancer and cachexia: results from a randomized, double-blind, placebo-controlled, multicenter study of Japanese patients (ONO-7643-04). *Cancer*. 2018;124:606-616.
10. Hamauchi S, Furuse J, Takano T, et al. A multicenter, open-label, single-arm study of anamorelin (ONO-7643) in advanced gastrointestinal cancer patients with cancer cachexia. *Cancer*. 2019;125:4294-4302.
11. Takayama K, Katakami N, Yokoyama T, et al. Anamorelin (ONO-7643) in Japanese patients with non-small cell lung cancer and cachexia: results of a randomized phase 2 trial. *Support Care Cancer*. 2016;24:3495-3505.
12. Latres E, Mastaitis J. Activin a more prominently regulates muscle mass in primates than does GDF8. *Nat Commun*. 2017;8:15153.
13. Walker RG, Poggioli T, Katsimpardi L, et al. Biochemistry and biology of GDF11 and myostatin: similarities, differences, and questions for future investigation. *Circ Res*. 2016;118:1125-1141.
14. Iskenderian A, Liu N, Deng Q, et al. Myostatin and activin blockade by engineered follistatin results in hypertrophy and improves dystrophic pathology in mdx mouse more than myostatin blockade alone. *Skelet Muscle*. 2018;8:34.
15. Grobet L, Martin LJ, Poncelet D, et al. A deletion in the bovine myostatin gene causes the double-muscling phenotype in cattle. *Nat Genet*. 1997;17:71-74.
16. Zhou X, Wang JL, Lu J, et al. Reversal of cancer cachexia and muscle wasting by ActRIIB antagonism leads to prolonged survival. *Cell*. 2010;142:531-543.
17. Morikawa M, Derynck R, Miyazono K. TGF- $\beta$  and the TGF- $\beta$  family: context-dependent roles in cell and tissue physiology. *Cold Spring Harb Perspect Biol*. 2016;8:a021873.
18. Ozawa T, Morikawa M, Morishita Y, et al. Systemic administration of monovalent follistatin-like 3-fc-fusion protein increases muscle mass in mice. *iScience*. 2021;24:102488.
19. Han HQ, Zhou X, Mitch WE, Goldberg AL. Myostatin/activin pathway antagonism: molecular basis and therapeutic potential. *Int J Biochem Cell Biol*. 2013;45:2333-2347.
20. Ojima C, Noguchi Y, Miyamoto T, et al. Peptide-2 from mouse myostatin precursor protein alleviates muscle wasting in cancer-associated cachexia. *Cancer Sci*. 2020;111:2954-2964.
21. Takayama K, Noguchi Y, Aoki S, et al. Identification of the minimum peptide from mouse myostatin prodomain for human myostatin inhibition. *J Med Chem*. 2015;58:1544-1549.
22. Takayama K, Asari T, Saitoh M, et al. Chain-shortened Myostatin inhibitory peptides improve grip strength in mice. *ACS Med Chem Lett*. 2019;10:985-990.
23. Saitoh M, Takayama K, Roppongi Y, et al. Strategic structure-activity relationship study on a follistatin-derived myostatin inhibitory peptide. *Bioorg Med Chem Lett*. 2021;46:128163.
24. Takayama K, Hitachi K, Okamoto H, et al. Development of myostatin inhibitory d-peptides to enhance the potency, increasing skeletal muscle mass in mice. *ACS Med Chem Lett*. 2022;13:492-498.

25. Miyake M, Hori S, Itami Y, et al. Supplementary oral anamorelin mitigates anorexia and skeletal muscle atrophy induced by gemcitabine plus cisplatin systemic chemotherapy in a mouse model. *Cancer*. 2020;12:1942.
26. Inman GJ, Nicolas FJ, Callahan JF, et al. SB-431542 is a potent and specific inhibitor of transforming growth factor-beta superfamily type I activin receptor-like kinase (ALK) receptors ALK4, ALK5, and ALK7. *Mol Pharmacol*. 2002;62:65-74.
27. Laping NJ, Grygielko E, Mathur A, et al. Inhibition of transforming growth factor (TGF)-beta1-induced extracellular matrix with a novel inhibitor of the TGF-beta type I receptor kinase activity: SB-431542. *Mol Pharmacol*. 2002;62:58-64.
28. Fukasawa K, Hanada K, Ichikawa K, et al. Endothelial-specific depletion of TGF- $\beta$  signaling affects lymphatic function. *Inflamm Regen*. 2021;41:35.
29. Itoh F, Itoh S, Adachi T, et al. Smad2/Smad3 in endothelium is indispensable for vascular stability via S1PR1 and N-cadherin expressions. *Blood*. 2012;119:5320-5328.
30. Jonk LJ, Itoh S, Heldin CH, ten Dijke P, Kruijjer W. Identification and functional characterization of a Smad binding element (SBE) in the JunB promoter that acts as a transforming growth factor-beta, activin, and bone morphogenetic protein-inducible enhancer. *J Biol Chem*. 1998;273:21145-21152.
31. Sabourin LA, Rudnicki MA. The molecular regulation of myogenesis. *Clin Genet*. 2000;57:16-25.
32. Keller-Pinter A, Szabo K, Kocsis T, et al. Syndecan-4 influences mammalian myoblast proliferation by modulating myostatin signaling and G1/S transition. *FEBS Lett*. 2018;592:3139-3151.
33. Milan G, Romanello V, Pescatore F, et al. Regulation of autophagy and the ubiquitin-proteasome system by the FoxO transcriptional network during muscle atrophy. *Nat Commun*. 2015;6:6670.
34. Hata A, Chen YG. TGF- $\beta$  signaling from receptors to Smads. *Cold Spring Harb Perspect Biol*. 2016;8:a022061.
35. Guttridge DC. A TGF- $\beta$  pathway associated with cancer cachexia. *Nat Med*. 2015;21:1248-1249.
36. Campbell C, McMillan HJ, Mah JK, et al. Myostatin inhibitor ACE-031 treatment of ambulatory boys with Duchenne muscular dystrophy: results of a randomized, placebo-controlled clinical trial. *Muscle Nerve*. 2017;55:458-464.
37. Lopez P, Newton RU, Taaffe DR, et al. Associations of fat and muscle mass with overall survival in men with prostate cancer: a systematic review with meta-analysis. *Prostate Cancer Prostatic Dis*. 2021. doi:10.1038/s41391-021-00442-0
38. Bozzetti F, Mori V. Nutritional support and tumour growth in humans: a narrative review of the literature. *Clin Nutr*. 2009;28:226-230.

#### SUPPORTING INFORMATION

Additional supporting information can be found online in the Supporting Information section at the end of this article.

**How to cite this article:** Hanada K, Fukasawa K, Hinata H, et al. Combination therapy with anamorelin and a myostatin inhibitor is advantageous for cancer cachexia in a mouse model. *Cancer Sci*. 2022;113:3547-3557. doi: [10.1111/cas.15491](https://doi.org/10.1111/cas.15491)